TECHNICAL ADVANCE

Image Analysis Workflow for 2-D Electrophoresis Gels Based on ImageJ

Massimo Natale[1,2], Bernardetta Maresca[3], Paolo Abrescia[3] and Enrico M. Bucci[1,4]

[1]BioDigitalValley S.r.l., via Carlo Viola 78, 11026 Pont Saint Martin (AO), Italy. [2]Department of Control and Computer Engineering, Politecnico di Torino, Turin, Italy. [3]Dipartimento delle Scienze Biologiche, Università di Napoli Federico II, Naples, Italy. [4]Istituto di Biostrutture e Bioimmagini, Via Mezzocannone 16, 80134, Naples, Italy.
Corresponding author email: enrico.bucci@biodigitalvalley.com

Abstract: A number of commercial software packages are currently available to perform digital two-dimensional electrophoresis (2D-GE) gel analysis. However, both the high cost of the commercial packages and the unavailability of a standard data analysis workflow, have prompted several groups to develop freeware systems to perform certain steps of gel analysis. Unfortunately, to the best of our knowledge none of them offer a package that performs all the steps envisaged in a 2D-GE gel analysis. Here we describe an ImageJ-based procedure, able to manage all the steps of a 2D-GE gel analysis. ImageJ is a free available image processing and analysis application developed by National Institutes of Health (NIH) and widely used in different life sciences fields as medical imaging, microscopy, western blotting and PAGE. Nevertheless no one has yet developed a procedure enabled to compare spots on 2D-GE gels. We collected all used ImageJ tools in a plug-in that allows us to perform the whole 2D-GE analysis. To test it, we performed a set of 2D-GE experiments on plasma samples from 9 patients victims of acute myocardial infarction and 8 controls, and we compared the results obtained by our procedure to those obtained using a widely diffuse commercial package, finding similar performances.

Keywords: 2-D gels, bioinformatics, image analysis, myocardial infarction, spot matching

Introduction

Two-dimensional gel electrophoresis (2D-GE) is a powerful technology to compare complex protein mixtures; it has been applied to many fields of biomedical research and is widely used in biomarker discovery. In a 2D-GE gel thousands of proteins are separated in well defined spots; these protein spots can be revealed via a variety of staining techniques (Coomassie, Silver Stain, Sypro),[1] and captured by one or more digitized computer images per gel(CCD camera, laser scanner, and optical scanner).[2] The image capturing phase transforms the biological information of the 2D-GE gel into a quantitative computer-readable data set. Once all the studied gels have been collected and digitized the software-based image analysis can be started. Image analysis is crucial in extracting biologically relevant information from a two-dimensional gel electrophoresis experiment.

Despite the availability of several software applications to analyze 2D-GE images, there is no general consensus on 2D-GE data analysis protocol. Moreover several authors reported that the commercial packages are time consuming, can often miss values or give false positives, and induce variance in quantitative measures.[3–9]

The commercially available software perform the analysis workflow in two different ways. The classical package condensed the information onto spots. The spot detection is performed prior to matching and expression profile extraction. The second image analysis software group is based on the whole image information. These packages apply a warping procedure to remove running differences between gels, and the spot detection and protein expression profiles extraction occurred in a separated and independent step.[5] The emphasis in this analysis software has been on reducing the subjectivity of the image analysis.

The fact that the alignment step is performed prior to the spot detection facilitates simultaneous spot detection on all gel images in an experiment and the resulting spot boundaries are identical on all gel images.[10] In Table 1 are collected the most popular commercial software for 2D-GE gel analysis.

Several research groups have developed freeware systems to handle certain key aspects of gel analysis, including archiving (SwissProt 2D),[11] comparison (Flicker),[12] interactive exploration (WebGel),[13] registration (bUnwarpJ and Sili2DGel),[14,15] spot detection,[16] spot quantification precision and differential expression (Pinnacle).[17] However nobody has developed a complete package freely available and platform independent able to perform all the steps of a 2D-GE gel analysis experiment.[18]

Leveraging also on these experiences we have developed an image analysis workflow based on the popular public domain image analysis software package ImageJ (http://rsb.info.nih.gov/ij/). ImageJ and its plug-in is easy-to-use software and can be used in routine applications. Our workflow has been developed according to the whole image information procedure.[19] It is based on six steps: aligning all the images, computing image fusion, creating a consensus spot pattern, propagating the consensus spot pattern to all gel images for quantification, and finally the statistic analysis.

In order to test our procedure, we performed a 2D-GE study of plasma from patients immediately after an acute myocardial event, comparing the results obtained using a widely diffused commercial package (Melanie; GeneBio, Geneva) to those obtained with our ImageJ-based procedure. We looked for biomarkers of pathology and/or treatment in acute myocardial infarction (AMI) patients treated with common anticoagulant protocols. The authors confirm that ethical approval was obtained for this research.

Table 1. The most popular commercial software for 2D-GE gel analysis.

Software package	Company	Type	Web link
PDQuest	BioRad, Hercules, CA	Spot based	www.bio-rad.com
ImageMaster 2D or DeCyder	GE Healthcare	Spot based	www.gehealthcare.com
Dymension	Syngene, Cambridge, UK	Spot based	www.syngene.com
Melanie	GeneBio, Geneva, Switzerland	Spot based	www.genebio.com
Delta2D	Decodon, Greifswald, Germany	Warping	www.decodon.com
Progenesis SameSpots	Nonlinear Dynamics, Newcastle, UK	Warping	www.nonlinear.com

Table 2. List of steps that describes how to perform the analysis.

Step	Description	Web link
1	Download and install ImageJ on your computer following the installation instructions specific to your platform (Windows, Mac OS, Linux, etc.);	http://rsbweb.nih.gov/ij/download.html
2	Align all images in pairs using bUnwarpJ plugin and taking always the same image as reference, and save the warped images;	http://biocomp.cnb.uam.es/~iarganda/bUnwarpJ/
3	Open all the warped images and save these in a stack as a sequence using the "Image>Stacks>Images To Stack command";	
4	Sum image using "Image>Stacks>Z Project...>Sum Slices";	
5	Perform spot detection on the fused image by the Watershed plug-in. Selected the binary output;	http://bigwww.epfl.ch/sage/soft/watershed/index.html
6	Apply the blob analyzer of ImageJ using "Analyze> Analyze Particles…", to measure the catchment basins and save the blots as a list of ROI;	
7	Open the stack image(saved in point 4) and propagated to all gel images the list of ROI obtained in by the spot detection procedure "ROI Manager>Show All";	
8	Measure the spots volume values using "ROI Manager>Measure" and save the Results as OpenOffice compatible (.ods) file;	http://www.openoffice.org
9	For quantitative comparison of spot intensities choose Integrated Density measure. This value is the integral of all pixel intensities within the spot boundary;	
10	Normalize the volume of each spot on a given gel image versus the total volume of all spots on that image, perform the ANOVA Test on normalized data.	

Material and Methods
2-DE page

With this aim, we enrolled 9 patients admitted within 6 hours after the onset of chest pain symptoms, with myocardial infarction defined according to ESC/ACC criteria. All subjects signed informed consent forms prior to standard sample collection. 2D-GE was performed according to Maresca et al[20] and each sample was run in duplicate. For the first-dimension electrophoresis of plasma samples 200 µg (approximately 3 µl) were applied to 18-cm linear IPG strips 4–7 GE Healthcare (Uppsala, Sweden) and focused until 72000 V/hr were reached. Prior to SDS-PAGE, the IPG strips were equilibrated twice for 15 min in equilibration buffer (50 mM Tris-HCl pH 8.8, 6 M urea, 30% (v/v) glycerol, 2% (w/v) SDS and traces of bromophenol blue) containing 1% (w/v) DTT for the first equilibration step and 2.5% (w/v) iodoacetamide for the second step. SDS-PAGE was performed on 12.5% polyacrylamide gels according to Laemmli.[21]

The run was carried out at 60 mA/gel at 16 °C and terminated when the dye front reached the lower end of the gel. Gels of plasma samples were visibly stained with Coomassie Blue, scanned using transmission mode to avoid saturation effects and saved in 16-bit TIFF format.

Image analysis

Once all gels in the study had been collected and digitalized, they were analyzed using the ImageJ and some of its plugins or the commercial software Melanie.

We now go through the ImageJ-based procedure, and then we will compare the results obtained to the Melanie output. In Table 2 is collected the list of steps that describes how to perform the analysis using ImageJ and its plug-in.

First, all images were warped by bUnwarpJ,[14] an algorithm for elastic and consistent image registration developed as an ImageJ plug-in. It performs a simultaneous registration of two images, allowing us to solve

the problem of spatial distortions due to run-time differences and dye-front deformations.

We used the software to align all images in pairs, taking always the same image as reference and producing the corresponding warped images of the others. bUnwarpJ can be freely downloaded from http://biocomp.cnb.uam.es/~iarganda/bUnwarpJ/.

The reference image and warped images were subsequently displayed in a single stack image and summed to generate a fused image. We followed an image sum approach to retain as much information as possible from the original images.

Spot detection was performed on the fused image by the watershed plug-in written by Daniel Sage and freely downloaded from http://bigwww.epfl.ch/sage/soft/watershed/index.html. This plug-in is able to segment an image using the watershed algorithm by flooding directly on graylevel image. Of the several kind of outputs provided, we selected the binary output that allows us to apply the blob analyzer of ImageJ, so as to measure the catchment basins and save the blots, one for each protein spot, as a list of regions of interest (ROI). Each ROI corresponds exactly to a spot in the fused image. The list of ROI obtained by the spot detection procedure was our consensus spot pattern that is valid for the whole gel set of the experiment.

In other words, the list of ROI obtained is equivalent to the grid used in gene chip analysis, this grid was imposed on each of the aligned gel images so that a defined number of areas were quantified on every gel image of the experiment. The spot volume values extracted from each image were listed in a ImageJ "Results table". The resulting table of "the whole image information procedure" did not have empty cells, while some commercial software, such as Melanie, are not able to eliminate all bias due to missing spot values.[22] All the data were analyzed by Calc (OpenOffice), a open source spreadsheet program downloadable from the web site http://www.openoffice.org/. For the normalization the volume of each spot on a given gel image was diveded by the total volume of all spots on that image.[23] The resulting table of our method did not have empty cells, while some commercial software, such as Melanie, are not able to eliminate all bias due to missing spot values.[22]

Results

The warping step has produced a good alignment of all 2D-GE images. In Figure 1 is shown an example
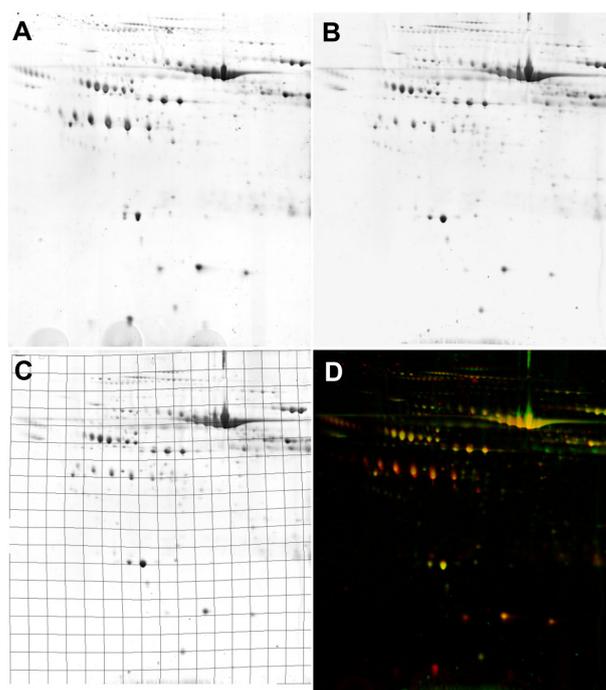
Figure 1. (**A** and **B**) shown two different 2D-GE images of two control subjects. In (**C**) is shown the elastic registration obtained during using bUnwarpJ plug-in. In Figure 1D is shown the overlap of the two gels after the warping step, in the red channel is shown the reference gel (Fig. 1A) and in the green channel is shown a warped gel.

of warping step results. Figure 1A and B show two different 2D-GE images, in Figure 1C is shown the elastic registration obtained during the warping, and in Figure 1D the overlap of the two gels after the warping step. For the image fusion process all the warped images were used and the fused images do not show multiple spots thanks to the strength of the elastic alignment.

Using the ImageJ procedure we were able to study 232 conserved spots, while with Melanie we analyzed
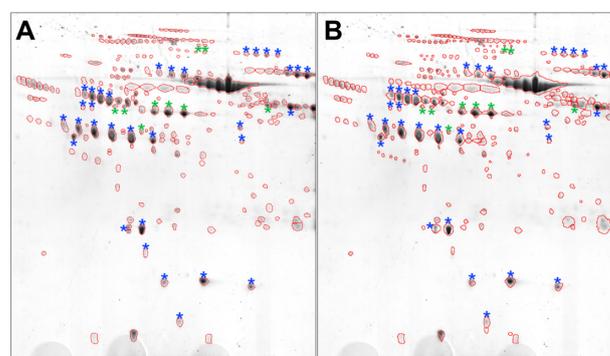
Figure 2. 2D-GE from the plasma of a control individual. (**A**) Spots detected and matched using Melanie. (**B**) Spots detected using the ImageJ procedure.
Note: The stars show the spots used for comparison of quantification methods (unchanged spots in blue, differential spots in green).
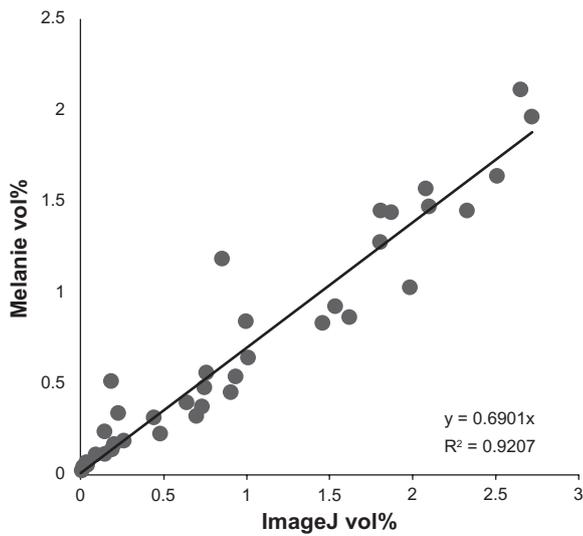
**Figure 3.** Scatter plot of spot mean volumes as evaluated by Melanie and ImageJ.
Notes: The ImageJ values are plotted on the X-axis, the Malenie values on the Y-axis. Spots were normalized based on total spot volume.

a pattern of 205 matched spots. The spot detection and the matching were manually checked in both the procedures; Figure 2 shows the spots detected by the two procedure on one of the control subject gels (the reference gel used for the Melanie analysis).

The scatter plot in Figure 3 shows that there is a linear relationship between the spot volumes evaluated by Melanie and the corresponding values obtained by the ImageJ procedure. In particular 42 spots, 33 more abundant spots (blue stars in Fig. 2) and the 9 differentially expressed spots (green stars in Fig. 2, see the next paragraph for the identification procedure) were considered for the comparison; the fact that the straight line in Figure 3 has a slope <1 means that volume values calculated for the same spot are on average larger by using the ImageJ procedure, which can be related to the slightly larger area segmented for each spot by ImageJ due to the fact that spots were segmented on the fused image (and not on every single gel, as Melanie does). Similar results were obtained for the spot list of every other gel as well as for the average volumes (data not shown).

The 9 differential spots (shown in Figure 4), whose mean normalized volume was significantly decreased in the myocardial infarction versus the control group, were all identified by t test (P-value <0.001); the test was run independently on the list of the spots, quantified by our procedure or by Melanie. 7 out
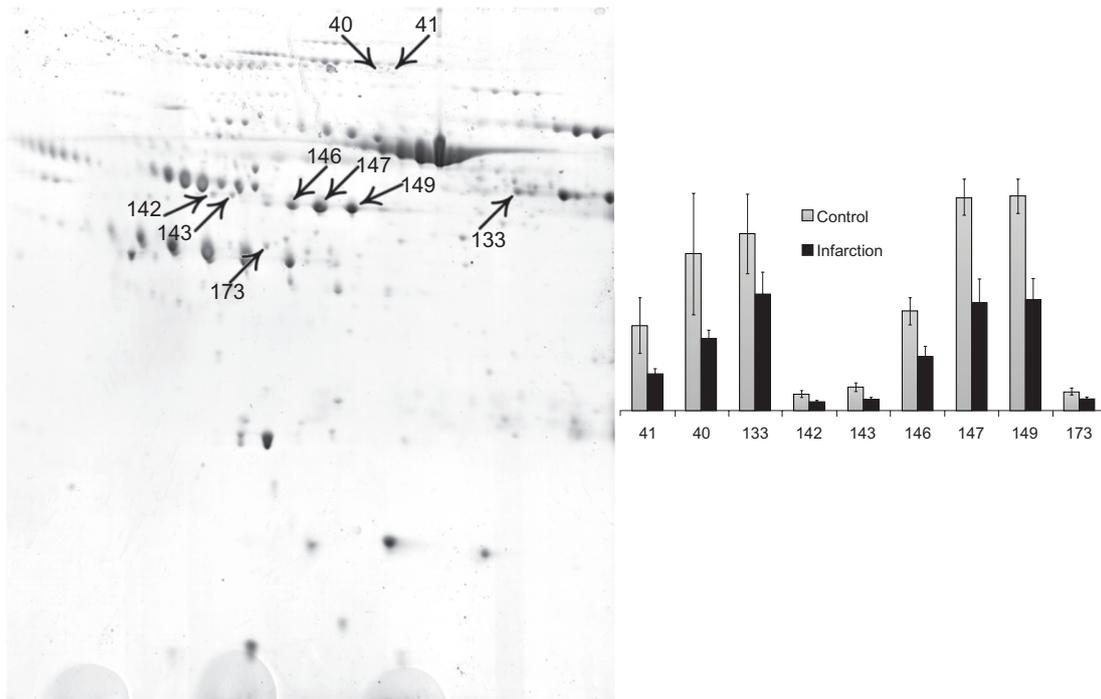
Figure 4. Profile of proteins differentially expressed in the plasma of myocardial infarction (MI) patients vs. control subjects. 7 spots were found significantly decreased in the plasma of the myocardial infarction patients by both methods (P-value < 0.001 , ANOVA test). Spots 133 and 173 were found to be differentially expressed by one method only (see text for explanation). Spots 142, 143, 146, 147 and 149 were identified as fibrinogen gamma chain fragments. In supplementary materials is shown the table with all raw data of the spots.

of the 9 spots were well above the selected *P*-value threshold for both Melanie and the ImageJ-based procedure, while each of the 2 methods identified an additional spot which was missed by the other (with reference to Figure 4, spots 133 and 173 where identified only by Melanie and ImageJ respectively). These 2 spots have a *P*-value slightly higher than the threshold and anyway with a significance under 0.05. All data of the spots are shown in table in supplementary material.

By using the procedure described by Lemkin et al,[24] ie, by matching the spots of a gel with those of a reference map of human plasma (http://expasy.org/swiss-2dpage/viewer), we were able to tentatively identify 5 of the 7 significantly different spots as fibrinogen gamma chain fragments (with reference to Figure 4, spots 142, 143, 146, 147, and 148).

Discussion and Conclusions

Previous proteomic studies reported protein expression differences in plasma from patients during an acute coronary syndrome and from patients with moderate hypercholesterolemia,[25] and proteomic differences in the plasma of coronary ischemic patients resistant to aspirin as compared to aspirin-sensitive patients.[26] Interestingly, 3 of the very same gamma fibrinogen spots were reported as increased in untreated myocardial infarction,[25] but thrombolytic (fibrinolytic) therapy reduces the level of all fibrinogen chains (see for example[27]). Since all the enrolled patients received an anticoagulant therapy, this decrease is possibly connected to the therapy, and thus may reflect modifications of the fibrin/fibrinogen balance in the patient blood.

Further experimental work in a larger patient cohort will be needed to confirm these data, and the study of the effects of anticoagulant therapy on hospitalized patients goes beyond the purpose of this work.

In conclusion, we have developed a free and easy alternative to a common commercial package for the segmentation and quantification of 2D gel spots; the procedure proved to be so effective, to confirm the results obtained by an established commercial solution.

We hope that the provided solution can help proteomic laboratories to quickly and inexpensively evaluate 2D-gel experimental results, without losing the required accuracy and providing a common reference for future analyses.

Acknowledgements

Disclosures

References

1. Beat MR. Non-covalent and covalent protein labeling in two-dimensional gel electrophoresis. *Journal of Proteomics*. July 21, 2008;71(2):231–44.
2. Natasha AK, Renata F, Denis VR, Kathryn SL. Comparison of DIGE and post-stained gel electrophoresis with both traditional and SameSpots analysis for quantitative proteomics. *Proteomics*. March 5, 2008;8(5):948–60.
3. Millioni R, Sbrignadello S, Tura A, Iori E, Murphy E, Tessari P. The inter- and intra-operator variability in manual spot segmentation and its effect on spot quantitation in two-dimensional electrophoresis analysis. *Electrophoresis*. May 2010;31(10):1739–42.
4. Millioni R, Miuzzo M, Sbrignadello S, et al. Delta2D and Proteomweaver: Performance evaluation of two different approaches for 2-DE analysis. *Electrophoresis*. Apr 2010;31(8):1311–7.
5. Berth M, Moser FM, Kolbe M, Bernhardt J. The state of the art in the analysis of two-dimensional gel electrophoresis images. *Appl Microbiol Biotechnol*. 2007;76:1223–43.
6. Millioni R, Sbrignadello S, Tura A, Iori E, Murphy E, Tessari P. The inter- and intra-operator variability in manual spot segmentation and its effect on spot quantitation in two-dimensional electrophoresis analysis. *Electrophoresis*. May 31, 2010;10:1739–42.
7. Kang Y, Techanukul T, Mantalaris A, Nagy JM. Comparison of three commercially available DIGE analysis software packages: minimal user intervention in gel-based proteomics. *J Proteome Res*. 2009;8(2):1077–84.
8. Clark BN, Gutstein HB. The myth of automated, high-throughput two-dimensional gel analysis. *Proteomics*. Mar 2008;8(6):1197–203.
9. Wheelock AM, Buckpitt AR. Software-induced variance in two-dimensional gel electrophoresis image analysis. *Electrophoresis*. 2005;26:4508–20.
10. Dowsey AW, Morris JS, Gutstein HB, Yang GZ. Informatics and statistics for analyzing 2-d gel electrophoresis images. *Methods Mol Biol*. 2010;604:239–55.

11. Appel RD, Hoogland C, Bairoch A, Hochstrasser DF. Constructing a 2-D database for the World Wide Web. *Methods Mol Biol*. 1999;112:411–6.
12. Lemkin PF. Comparing two-dimensional electrophoretic gel images across the Internet. *Electrophoresis*. Mar-Apr 1997;18(3–4):461–70.
13. Lemkin PF, Myrick JM, Lakshmanan Y, et al. Exploratory data analysis groupware for qualitative and quantitative electrophoretic gel analysis over the Internet-WebGel. *Electrophoresis*. Dec 1999;20(18):3492–507.
14. Sorzano CO, Arganda-Carreras I, Thévenaz P, et al. Elastic image registration of 2-D gels for differential and repeatability studies. *Proteomics*. 2008; 8:62–5.
15. Pérès S, Molina L, Salvetat N, Granier C, Molina F. A new method for 2D gel spot alignment: application to the analysis of large sample sets in clinical proteomics. *BMC Bioinformatics*. October 28, 2008;9:460.
16. dos Anjos A, Møller AL, Ersbøll BK, Finnie C, Shahbazkia HR. New approach for segmentation and quantification of two-dimensional gel electrophoresis images. *Bioinformatics*. February 1, 2011;27(3):368–75. Epub Dec 2, 2010.
17. Morris JS, Clark BN, Wei W, Gutstein HB. Evaluating the performance of new approaches to spot quantification and differential expression in 2-dimensional gel electrophoresis studies. *J Proteome Res*. 2010;9: 595–604.
18. Marengo E, Robotti E, Antonucci F, Cecconi D, et al, Numerical approaches for quantitative analysis of two-dimensional maps: a review of commercial software and home-made systems. *Proteomics*. 2005;5:654–66.
19. Bandow JE, Baker JD, Berth M, Painter C. Improved image analysis workflow for 2-D gels enables large-scale 2-D gel-based proteomics studies—COPD biomarker discovery study. *Proteomics*. 2008;8:3030–41.
20. Maresca B, Cigliano L, Corsaro MM, et al. Current Quantitative determination of haptoglobin glycoform variants in psoriasis. *Biol .Chem*. Dec 2010;391(12):1429–39.
21. Laemmli UK. Cleavage of structural proteins during the assembly of the head of bacteriophage T4. *Nature*. 1970;227(5259):680–5.
22. Chang J, Van Remmen H, Ward WF, Regnier FE, Richardson A, Cornell J. Processing of data generated by 2-dimensional gel electrophoresis for statistical analysis: missing data, normalization, and statistics. *J Proteome Res*. 2004;3:1210–8.
23. Nishihara JC, Champion KM. Quantitative evaluation of proteins in one- and two-dimensional polyacrylamide gels using a fluorescent stain. *Electrophoresis*. July 23, 2002;(14):2203–15.
24. Lemkin PF, Thornwall G. Flicker image comparison of 2-D gel images for putative protein identification using the 2DWG meta-database. *Mol Biotechnol*. Sep 1999;12(2):159–72.
25. Mateos-Cáceres PJ, García-Méndez A, López Farré A, et al. Proteomic analysis of plasma from patients during an acute coronary syndrome. *JACC*. October 19, 2004;44(8):1578–83.
26. López-Farré AJ, Mateos-Cáceres PJ, Sacristán D, et al. Relationship between vitamin D binding protein and aspirin resistance in coronary ischemic patients: a proteomic study. *Journal of Proteome Research*. 2007;6:2481–7.
27. Rao AK, Pratt C, Berke A, et al. Thrombolysis in Myocardial Infarction (TIMI) Trial—phase I: hemorrhagic manifestations and changes in plasma fibrinogen and the fibrinolytic system in patients treated with recombinant tissue plasminogen activator and streptokinase. *J Am Coll Cardiol*. Jan 1988;11(1):1–11.

Supplementary Materials

The table shows the data obtained for ImageJ based analysis. The spots in green have a *P*-value < 0.001 (these spots are shown in Fig. 3). In yellow is shown the spot 173, this spot has a *P*-value < 0.05 in ImageJ analysis and *P*-value < 0.001 in Melanie analysis (this spot is shown in Fig. 3).

	Control mean	Control St_Dev	Control median	Infarction mean	Infarction St_Dev	Infartion median	T test *P*-value	Wilcoxon *P*-value
149	1.401	0.114	1.421	0.721	0.146	0.705	0.0000001	0
147	1.394	0.117	1.355	0.702	0.155	0.656	0.0000001	0
146	0.653	0.092	0.656	0.351	0.068	0.329	0.0000179	0
143	0.154	0.028	0.148	0.071	0.016	0.066	0.0000692	0
41	0.016	0.005	0.013	0.007	0.001	0.007	0.0001684	0
142	0.107	0.022	0.096	0.055	0.010	0.051	0.0004514	0
133	0.124	0.023	0.118	0.076	0.015	0.067	0.0006462	0
40	0.029	0.011	0.024	0.013	0.002	0.013	0.0009521	0
79	0.052	0.014	0.054	0.025	0.009	0.022	0.0020000	0.0020000
154	0.196	0.018	0.191	0.150	0.031	0.158	0.0020000	0.0020000
135	1.156	0.258	1.180	0.759	0.144	0.771	0.0050000	0.0040000
173	0.119	0.040	0.137	0.059	0.024	0.051	0.0060000	0.0120000
144	0.018	0.004	0.017	0.013	0.002	0.012	0.0070000	0.0000000
157	0.006	0.001	0.006	0.005	0.001	0.005	0.0070000	0.0060000
25	0.151	0.059	0.164	0.218	0.031	0.219	0.0250000	0.0120000
124	0.352	0.043	0.365	0.297	0.046	0.300	0.0260000	0.0320000
199	0.019	0.006	0.016	0.027	0.005	0.027	0.0260000	0.0320000
4	0.093	0.034	0.075	0.130	0.025	0.131	0.0340000	0.0420000
150	0.386	0.106	0.359	0.277	0.057	0.266	0.0390000	0.0080000
182	0.197	0.018	0.199	0.221	0.024	0.211	0.0430000	0.0900000
224	0.175	0.031	0.165	0.141	0.030	0.153	0.0450000	0.0420000
22	0.191	0.085	0.206	0.273	0.049	0.255	0.0490000	0.0540000
1	0.036	0.011	0.032	0.054	0.021	0.050	0.0550000	0.0720000
177	0.461	0.096	0.463	0.626	0.212	0.676	0.0610000	0.1420000
129	0.135	0.051	0.114	0.189	0.058	0.185	0.0660000	0.0720000
5	0.065	0.024	0.052	0.088	0.024	0.090	0.0780000	0.0900000
183	0.202	0.011	0.203	0.226	0.034	0.224	0.0800000	0.2100000
46	0.034	0.011	0.034	0.024	0.010	0.021	0.0810000	0.0420000
21	0.227	0.104	0.251	0.320	0.088	0.334	0.0820000	0.1740000
2	0.087	0.030	0.073	0.115	0.029	0.113	0.0830000	0.0900000
223	0.025	0.005	0.024	0.042	0.026	0.029	0.0860000	0.0220000
103	0.439	0.036	0.452	0.402	0.046	0.400	0.0950000	0.1420000
73	0.469	0.133	0.484	0.606	0.179	0.555	0.1030000	0.0900000
165	0.128	0.047	0.105	0.205	0.119	0.140	0.1040000	0.1140000
3	0.094	0.038	0.072	0.123	0.024	0.128	0.1090000	0.1740000
139	0.686	0.091	0.685	0.552	0.209	0.496	0.1110000	0.0900000
136	0.146	0.028	0.138	0.121	0.030	0.130	0.1140000	0.1740000
118	0.416	0.035	0.408	0.379	0.056	0.383	0.1220000	0.3000000
110	0.087	0.009	0.084	0.079	0.010	0.079	0.1280000	0.1420000
43	0.006	0.005	0.003	0.002	0.000	0.002	0.1300000	0.0120000

(*Continued*)

(*Continued*)

	Control mean	Control St_Dev	Control median	Infarction mean	Infarction St_Dev	Infartion median	T test *P*-value	Wilcoxon *P*-value
74	1.095	0.279	1.187	1.341	0.332	1.273	0.1300000	0.2520000
122	0.018	0.003	0.017	0.015	0.003	0.015	0.1300000	0.1140000
170	0.028	0.002	0.028	0.041	0.023	0.033	0.1340000	0.1420000
54	0.010	0.002	0.009	0.012	0.003	0.012	0.1360000	0.1140000
60	0.052	0.010	0.052	0.060	0.011	0.062	0.1360000	0.2100000
163	0.155	0.014	0.157	0.142	0.020	0.142	0.1420000	0.2100000
44	0.007	0.006	0.003	0.003	0.000	0.003	0.1480000	0.1140000
78	0.077	0.023	0.082	0.110	0.058	0.128	0.1480000	0.2100000
86	0.007	0.001	0.007	0.008	0.002	0.008	0.1540000	0.2100000
141	0.078	0.072	0.042	0.033	0.012	0.028	0.1540000	0.3520000
42	0.009	0.008	0.004	0.004	0.001	0.004	0.1570000	0.2520000
219	0.244	0.031	0.233	0.201	0.077	0.164	0.1570000	0.0720000
6	0.023	0.008	0.020	0.029	0.008	0.030	0.1590000	0.1740000
30	0.064	0.025	0.066	0.087	0.038	0.079	0.1590000	0.2100000
29	0.114	0.041	0.127	0.144	0.037	0.153	0.1610000	0.1740000
168	0.036	0.013	0.035	0.054	0.034	0.044	0.1660000	0.1420000
39	0.016	0.004	0.014	0.014	0.003	0.014	0.1730000	0.3520000
47	0.088	0.027	0.077	0.111	0.038	0.100	0.1740000	0.3000000
178	0.025	0.006	0.027	0.029	0.006	0.029	0.1780000	0.1740000
121	0.347	0.112	0.336	0.421	0.102	0.420	0.1970000	0.1740000
115	1.627	0.167	1.669	1.733	0.147	1.691	0.2090000	0.3000000
231	0.043	0.012	0.040	0.091	0.104	0.041	0.2120000	0.5360000
58	0.078	0.024	0.079	0.061	0.027	0.057	0.2130000	0.1740000
137	0.050	0.041	0.033	0.028	0.013	0.021	0.2140000	0.2520000
15	0.029	0.026	0.018	0.046	0.028	0.035	0.2170000	0.1740000
215	0.614	0.039	0.597	0.579	0.069	0.587	0.2200000	0.2520000
111	0.164	0.030	0.152	0.141	0.041	0.132	0.2280000	0.1740000
123	0.208	0.028	0.217	0.232	0.048	0.211	0.2340000	0.7580000
172	0.359	0.133	0.391	0.286	0.091	0.300	0.2370000	0.2520000
229	0.183	0.138	0.095	0.106	0.096	0.075	0.2380000	0.6060000
159	0.037	0.008	0.036	0.044	0.013	0.043	0.2410000	0.3000000
200	0.100	0.055	0.110	0.073	0.025	0.063	0.2490000	0.5360000
228	0.528	0.225	0.587	0.659	0.203	0.681	0.2500000	0.2100000
48	0.192	0.056	0.174	0.222	0.041	0.217	0.2580000	0.1740000
195	0.017	0.002	0.017	0.023	0.016	0.017	0.2590000	0.3000000
107	0.049	0.011	0.045	0.044	0.003	0.044	0.2650000	0.6800000
131	0.595	0.075	0.577	0.652	0.123	0.673	0.2700000	0.1140000
102	0.172	0.026	0.181	0.160	0.014	0.160	0.2710000	0.2520000
20	0.289	0.133	0.270	0.360	0.109	0.362	0.2720000	0.4080000
19	0.217	0.116	0.206	0.276	0.074	0.269	0.2740000	0.3520000
76	0.028	0.009	0.028	0.032	0.007	0.033	0.2780000	0.6060000
98	0.453	0.088	0.456	0.498	0.064	0.515	0.2790000	0.3000000
184	0.058	0.023	0.053	0.046	0.015	0.049	0.2890000	0.2520000
132	0.275	0.063	0.291	0.246	0.031	0.258	0.2900000	0.3000000
160	0.013	0.002	0.013	0.015	0.004	0.016	0.2990000	0.3520000
210	0.016	0.001	0.016	0.019	0.007	0.016	0.3020000	0.6800000
188	0.200	0.035	0.205	0.179	0.044	0.200	0.3130000	0.4080000

(*Continued*)

(*Continued*)

	Control mean	Control St_Dev	Control median	Infarction mean	Infarction St_Dev	Infartion median	T test *P*-value	Wilcoxon *P*-value
7	0.039	0.016	0.042	0.046	0.014	0.049	0.3260000	0.2520000
31	0.023	0.009	0.026	0.027	0.007	0.029	0.3380000	0.2520000
70	0.207	0.073	0.195	0.241	0.062	0.229	0.3380000	0.3000000
203	0.025	0.004	0.025	0.034	0.027	0.026	0.3400000	1.0000000
230	0.278	0.257	0.192	0.421	0.326	0.229	0.3440000	0.1740000
45	0.224	0.237	0.136	0.132	0.031	0.121	0.3470000	0.6060000
66	0.405	0.052	0.394	0.377	0.063	0.396	0.3480000	0.5360000
212	0.009	0.001	0.009	0.010	0.003	0.009	0.3490000	0.5360000
10	0.114	0.057	0.122	0.137	0.025	0.141	0.3510000	0.4080000
67	1.791	0.326	1.845	1.975	0.436	1.851	0.3510000	0.4080000
57	0.016	0.007	0.015	0.013	0.004	0.013	0.3520000	0.4080000
130	0.090	0.012	0.090	0.083	0.015	0.089	0.3530000	0.6060000
164	0.043	0.004	0.046	0.045	0.007	0.045	0.3560000	0.4700000
11	0.101	0.050	0.107	0.121	0.026	0.118	0.3580000	0.4700000
82	0.019	0.018	0.013	0.012	0.002	0.012	0.3620000	0.5360000
27	0.005	0.001	0.005	0.005	0.001	0.005	0.3650000	0.3000000
117	0.238	0.063	0.243	0.280	0.115	0.259	0.3660000	0.6800000
65	0.239	0.076	0.249	0.268	0.031	0.264	0.3700000	0.4700000
204	0.062	0.014	0.068	0.055	0.020	0.056	0.3700000	0.4700000
64	0.105	0.029	0.097	0.116	0.012	0.115	0.3760000	0.3520000
96	0.230	0.042	0.223	0.246	0.027	0.245	0.3880000	0.2520000
8	0.055	0.025	0.061	0.066	0.019	0.069	0.3930000	0.4080000
55	37.791	2.655	38.727	39.108	3.319	39.207	0.3930000	0.6800000
9	0.091	0.045	0.097	0.108	0.025	0.120	0.3940000	0.3520000
214	1.888	0.160	1.946	1.793	0.271	1.846	0.3960000	0.3520000
33	0.068	0.026	0.075	0.078	0.014	0.077	0.3970000	0.6060000
201	0.020	0.006	0.019	0.026	0.019	0.020	0.3980000	0.7580000
53	0.015	0.005	0.012	0.017	0.005	0.017	0.4050000	0.5360000
221	0.153	0.019	0.149	0.143	0.030	0.135	0.4090000	0.1140000
13	0.036	0.031	0.024	0.049	0.032	0.036	0.4110000	0.4080000
56	0.023	0.009	0.024	0.019	0.007	0.018	0.4110000	0.4080000
227	0.457	0.236	0.447	0.364	0.191	0.370	0.4110000	0.6060000
80	0.177	0.048	0.165	0.160	0.021	0.161	0.4120000	0.5360000
104	0.043	0.007	0.044	0.040	0.007	0.041	0.4130000	0.3520000
151	0.300	0.162	0.246	0.244	0.082	0.226	0.4270000	0.5360000
12	0.087	0.042	0.084	0.101	0.021	0.101	0.4320000	0.3520000
89	0.066	0.031	0.053	0.056	0.017	0.050	0.4360000	0.3520000
209	0.018	0.001	0.018	0.020	0.006	0.018	0.4390000	1.0000000
232	0.043	0.056	0.021	0.026	0.011	0.022	0.4510000	0.6800000
94	0.667	0.141	0.668	0.716	0.102	0.767	0.4520000	0.4700000
51	0.128	0.057	0.126	0.109	0.039	0.112	0.4540000	0.5360000
114	1.760	0.348	1.904	1.873	0.238	1.887	0.4780000	0.6800000
26	0.049	0.019	0.043	0.043	0.012	0.043	0.4800000	0.7580000
208	0.211	0.034	0.206	0.223	0.032	0.227	0.4820000	0.6060000
72	0.085	0.032	0.083	0.095	0.016	0.091	0.4850000	0.2520000
38	0.005	0.002	0.005	0.004	0.001	0.004	0.4890000	0.9180000
108	1.147	0.336	1.278	1.253	0.226	1.254	0.4890000	0.7580000

(*Continued*)

(*Continued*)

	Control mean	Control St_Dev	Control median	Infarction mean	Infarction St_Dev	Infartion median	T test *P*-value	Wilcoxon *P*-value
77	0.897	0.118	0.914	0.951	0.195	0.937	0.5030000	0.6800000
197	0.014	0.004	0.015	0.013	0.002	0.013	0.5060000	0.4700000
207	0.019	0.004	0.019	0.018	0.005	0.017	0.5080000	0.5360000
34	0.050	0.020	0.062	0.056	0.013	0.058	0.5180000	0.6800000
125	0.044	0.006	0.047	0.046	0.006	0.045	0.5210000	0.8380000
156	0.026	0.005	0.025	0.032	0.026	0.022	0.5220000	0.5360000
88	0.296	0.091	0.265	0.273	0.033	0.272	0.5290000	1.0000000
218	1.225	0.365	1.215	1.125	0.192	1.101	0.5290000	0.6060000
18	0.132	0.065	0.133	0.150	0.035	0.150	0.5370000	0.7580000
153	0.018	0.004	0.016	0.016	0.003	0.017	0.5370000	0.4700000
206	0.207	0.056	0.196	0.189	0.052	0.193	0.5370000	0.6060000
158	0.205	0.044	0.186	0.222	0.061	0.234	0.5380000	0.3000000
155	0.107	0.025	0.098	0.099	0.024	0.102	0.5470000	0.7580000
93	0.954	0.218	0.873	1.014	0.153	1.101	0.5520000	0.5360000
190	0.015	0.005	0.015	0.016	0.005	0.015	0.5550000	0.7580000
92	0.195	0.084	0.164	0.175	0.024	0.169	0.5580000	0.8380000
32	0.046	0.016	0.051	0.050	0.013	0.056	0.5610000	0.4080000
116	0.074	0.008	0.074	0.078	0.020	0.081	0.5640000	0.4080000
225	1.178	0.652	1.517	0.993	0.659	1.110	0.5840000	0.7580000
52	0.010	0.004	0.008	0.012	0.005	0.011	0.5910000	0.6060000
24	0.025	0.009	0.023	0.022	0.005	0.023	0.5920000	0.7580000
87	0.215	0.070	0.204	0.199	0.040	0.190	0.5960000	0.6800000
176	0.220	0.029	0.227	0.231	0.051	0.216	0.5980000	0.8380000
120	0.164	0.039	0.160	0.154	0.031	0.139	0.6020000	0.5360000
14	0.057	0.026	0.055	0.062	0.011	0.062	0.6030000	0.6060000
71	0.699	0.071	0.686	0.675	0.110	0.684	0.6070000	0.6800000
23	0.081	0.025	0.084	0.087	0.014	0.085	0.6180000	0.5360000
191	0.011	0.003	0.011	0.012	0.003	0.012	0.6200000	0.6800000
140	0.075	0.051	0.046	0.063	0.040	0.038	0.6240000	0.9180000
187	0.131	0.037	0.127	0.141	0.035	0.150	0.6280000	0.5360000
75	1.820	0.202	1.802	1.741	0.450	1.728	0.6470000	0.9180000
16	0.044	0.018	0.048	0.047	0.008	0.046	0.6480000	1.0000000
37	0.053	0.013	0.054	0.051	0.009	0.049	0.6480000	0.4700000
167	0.076	0.020	0.079	0.081	0.019	0.082	0.6480000	0.4700000
222	0.059	0.018	0.054	0.063	0.011	0.058	0.6480000	0.3000000
68	0.230	0.072	0.238	0.244	0.034	0.240	0.6540000	0.8380000
194	0.041	0.011	0.041	0.044	0.010	0.043	0.6570000	0.6060000
217	2.982	0.719	3.044	2.837	0.501	2.737	0.6580000	0.6060000
91	0.142	0.068	0.115	0.130	0.023	0.129	0.6600000	0.6060000
181	0.392	0.109	0.425	0.368	0.100	0.343	0.6600000	0.6800000
192	0.025	0.007	0.023	0.026	0.006	0.026	0.6630000	0.5360000
126	1.043	0.241	1.040	0.996	0.177	1.068	0.6700000	1.0000000
84	0.024	0.005	0.024	0.025	0.005	0.023	0.6720000	1.0000000
106	0.403	0.071	0.395	0.388	0.064	0.412	0.6720000	0.7580000
97	1.123	0.287	1.052	1.175	0.179	1.200	0.6840000	0.5360000
83	0.012	0.002	0.012	0.011	0.002	0.010	0.6860000	0.9180000
152	0.430	0.111	0.394	0.411	0.066	0.391	0.6920000	0.9180000

(*Continued*)

(*Continued*)

	Control mean	Control St_Dev	Control median	Infarction mean	Infarction St_Dev	Infartion median	T test *P*-value	Wilcoxon *P*-value
161	0.090	0.032	0.071	0.096	0.031	0.099	0.6970000	0.7580000
119	0.822	0.194	0.750	0.854	0.093	0.856	0.7060000	0.2100000
105	0.541	0.229	0.496	0.578	0.134	0.574	0.7090000	0.5360000
185	0.042	0.007	0.041	0.043	0.010	0.042	0.7090000	0.6800000
61	0.120	0.020	0.123	0.116	0.022	0.120	0.7140000	0.9180000
220	0.112	0.022	0.116	0.118	0.040	0.127	0.7140000	0.8380000
134	0.142	0.117	0.074	0.121	0.116	0.085	0.7300000	0.7580000
202	0.111	0.039	0.104	0.117	0.021	0.113	0.7310000	0.8380000
99	1.134	0.315	1.046	1.182	0.207	1.137	0.7350000	0.3520000
50	0.022	0.007	0.022	0.021	0.007	0.021	0.7400000	0.6060000
162	0.589	0.144	0.523	0.620	0.233	0.657	0.7430000	0.9180000
85	0.038	0.012	0.035	0.037	0.008	0.033	0.7500000	0.9180000
101	0.014	0.004	0.014	0.014	0.002	0.014	0.7530000	0.9180000
28	0.035	0.012	0.037	0.033	0.011	0.030	0.7660000	1.0000000
100	0.032	0.016	0.029	0.034	0.008	0.033	0.7840000	0.1740000
186	0.022	0.008	0.022	0.023	0.007	0.024	0.7850000	0.6060000
211	0.016	0.001	0.016	0.017	0.002	0.016	0.7850000	0.9180000
90	0.283	0.092	0.245	0.273	0.042	0.269	0.7940000	0.8380000
128	0.807	0.130	0.812	0.825	0.142	0.866	0.7960000	0.6800000
213	0.059	0.018	0.060	0.057	0.012	0.057	0.7980000	0.9180000
145	0.030	0.017	0.022	0.032	0.013	0.027	0.8040000	0.4700000
17	0.064	0.029	0.070	0.067	0.014	0.062	0.8120000	0.9180000
95	0.154	0.059	0.134	0.160	0.033	0.154	0.8180000	0.3520000
196	0.030	0.009	0.028	0.029	0.009	0.033	0.8190000	0.6800000
169	1.648	0.335	1.560	1.601	0.500	1.717	0.8260000	1.0000000
148	0.010	0.004	0.009	0.010	0.004	0.010	0.8560000	0.7580000
205	0.025	0.009	0.024	0.024	0.004	0.024	0.8710000	0.6800000
59	0.416	0.120	0.431	0.424	0.064	0.406	0.8750000	0.6060000
63	0.005	0.001	0.005	0.005	0.001	0.005	0.8780000	1.0000000
62	0.087	0.017	0.084	0.086	0.011	0.088	0.8870000	0.9180000
109	0.012	0.002	0.011	0.012	0.002	0.012	0.9250000	1.0000000
179	0.133	0.020	0.137	0.131	0.030	0.133	0.9270000	0.9180000
127	0.715	0.125	0.745	0.719	0.111	0.689	0.9410000	1.0000000
216	0.015	0.006	0.013	0.015	0.004	0.014	0.9420000	0.8380000
174	0.372	0.024	0.375	0.373	0.048	0.359	0.9480000	1.0000000
69	0.036	0.014	0.039	0.036	0.007	0.033	0.9580000	0.8380000
112	0.158	0.021	0.153	0.157	0.044	0.159	0.9610000	0.7580000
193	0.040	0.010	0.042	0.040	0.009	0.041	0.9610000	0.9180000
171	1.646	0.348	1.625	1.655	0.481	1.882	0.9660000	0.5360000
189	0.160	0.065	0.154	0.158	0.037	0.170	0.9660000	0.6060000
226	0.229	0.112	0.242	0.226	0.197	0.139	0.9660000	0.7580000
166	1.161	0.242	1.068	1.155	0.439	1.272	0.9730000	0.8380000
198	0.035	0.009	0.035	0.035	0.008	0.032	0.9760000	1.0000000
49	0.216	0.067	0.231	0.215	0.035	0.221	0.9800000	0.7580000
81	0.014	0.003	0.014	0.014	0.003	0.014	0.9810000	1.0000000
113	0.094	0.022	0.084	0.094	0.020	0.096	0.9820000	0.6800000
175	1.092	0.274	1.065	1.089	0.311	1.055	0.9830000	1.0000000

(*Continued*)

(*Continued*)

	Control mean	Control St_Dev	Control median	Infarction mean	Infarction St_Dev	Infarction median	T test *P*-value	Wilcoxon *P*-value
180	0.077	0.011	0.080	0.077	0.012	0.080	0.9830000	0.9180000
36	0.036	0.011	0.036	0.036	0.008	0.035	0.9950000	1.0000000
138	0.489	0.104	0.431	0.489	0.109	0.447	0.9970000	0.7580000
35	0.020	0.009	0.015	0.020	0.007	0.018	0.9980000	0.8380000